On the role of secondary pions in spallation targets

Davide Mancusi[1,a], Sergio Lo Meo[2,4], Nicola Colonna[3], and Cristian Massimi[4]

[1] CEA, Paris-Saclay, 91191 Gif-sur-Yvette, France
[2] ENEA, Research Centre "Ezio Clementel", 40129 Bologna, Italy
[3] INFN, Section of Bari, 70125 Bari, Italy
[4] INFN, Section of Bologna, 40127 Bologna, Italy

Abstract. We use particle-transport simulations to show that secondary pions play a crucial role for the development of the hadronic cascade and therefore for the production of neutrons and photons from a thick spallation target. Considering the spallation target of the n_TOF Facility at CERN, we see that photon and neutron yields are relatively insensitive to large changes of the average pion multiplicity in the individual spallation reactions. We characterize this robustness as a peculiar property of hadronic cascades in thick targets.

1. Introduction

In spallation reactions, a high-energy ($>$ 150 MeV) light projectile collides with a nucleus and on average leads to the emission of a large number of particles, mostly neutrons.

The standard theoretical tool for the description of spallation reactions is a hybrid nuclear-reaction model where an intranuclear-cascade (INC) stage is followed by a statistical de-excitation stage [1].

Several spallation neutron sources are currently operational around the world and more are under construction or planned for the near future. Among the currently operating spallation neutron sources, the n_TOF (neutron Time-Of-Flight) facility [2] is an intense pulsed neutron source located at CERN.

In recent publications [3,4], the Geant4 toolkit for particle transport [5,6] was used to characterize the neutron and photon fluxes directed towards the n_TOF experimental areas. Calculations of neutron and photon fluences performed with different Geant4 physics lists exhibited large relative differences. The authors suggested at the time that this difference could be related to different treatments of pion production and pion-induced reactions.

In this work, we study the role of pion production and its influence on the spallation yields.

2. The Liège Intranuclear Cascade model

The Liège Intranuclear Cascade model (INCL) [7,8] is one of the most refined existing tools for the description of spallation reactions. The model is currently maintained and developed jointly by the University of Liège (Belgium) and CEA (Saclay, France). The model assumes that the first stage of the reaction can be described as an avalanche of independent binary collisions.

Intranuclear-cascade models in general (and INCL in particular) only describe the fast, dynamical stage of a spallation reaction, leading to the formation of equilibrated, excited nuclei which subsequently de-excite by particle emission and/or fission. It is therefore necessary to follow the de-excitation of this cascade *remnant* if one requires a complete description of the nuclear reaction.

In nuclear-reaction codes, de-excitation is commonly simulated by statistical de-excitation models. Within Geant4, INCL can be coupled with two different de-excitation codes, namely: G4ExcitationHandler, the native statistical de-excitation model of Geant4 and the default choice [9], and ABLA V3, a de-excitation model developed at GSI (Darmstadt, Germany) [10,11]. Different particles are produced in different stages of the spallation reactions. In particular, while neutrons and γ-rays are mostly generated in de-excitation processes, pion production, in particular, occurs entirely in the first reaction stage. The pion dynamics in INCL has been recently upgraded to push the upper energy limit of the model up to 15–20 GeV.

Older versions of INCL considered only one mechanism for pion production, namely excitation and subsequent decay of the $\Delta(1232)$ resonance. In the latest version of the INCL model, the production and decay of individual resonances (except for $\Delta(1232)$) is bypassed and replaced by *multipion collisions*, i.e. effective two-body collisions leading to the production of one or more pions in the final state.

Figure 1 shows the average pion multiplicity (i.e. the average number of pions produced per inelastic reaction) in p+^{208}Pb as a function of the proton energy. While the two models yield similar predictions at low projectile energy, in the older model the multiplicity saturates around 5 GeV, never exceeding $\sim$ 1 pion per reaction, while the extended model yields an almost linear increase up to 20 GeV.

2.1. Thin target: Pion-production cross sections

In order to assess the validity of the INCL++ and other models, it is very useful to compare with one of the most complete and comprehensive data set on pion

[a] e-mail: davide.mancusi@cea.fr

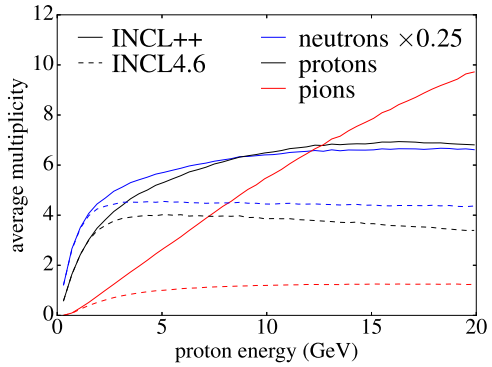

Figure 1. Excitation function for the average neutron, proton and pion multiplicities in the final state of p+^{208}Pb reactions, as calculated with (INCL++) and without (INCL4.6) multipion extension. Note that the neutron curve has been renormalized by a factor of 0.25.

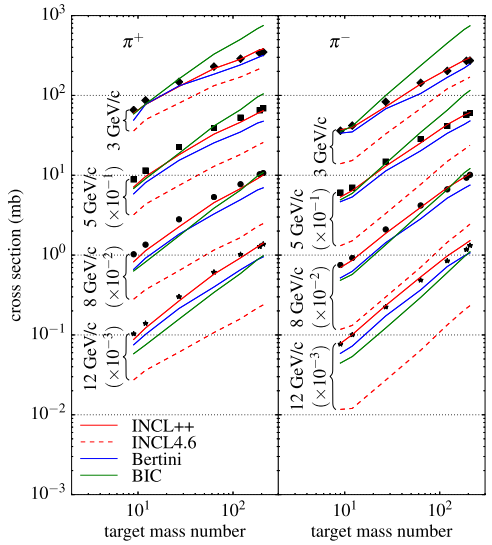

Figure 2. Cross sections for the production of π^+ (left) and π^- (right) from proton-nucleus reactions, integrated over the HARP angle-momentum acceptance, for different incident proton momenta, as a function of the target mass number. The lines represent calculations by different models (see text for details). The experimental data are taken from Ref. [12].

production at high energy. Such data were collected by the HARP experiment at CERN [12,13], where extensive measurements of double-differential cross sections for charged-pion production in proton- and pion-induced reactions were performed. Incident momenta of 3, 5, 8 and 12 GeV/c were considered.

Figure 2 shows inclusive pion-production cross sections integrated over the acceptance of the HARP experiment. In addition to the INCL++ calculation, we show the results of three other models: BERTINI [14] and Binary Cascade (BIC) [15] are popular intranuclear-cascade models available in Geant4, while INCL4.6 represents the INCL model *without* multipion extension [16].

As shown the INCL++ and BERTINI models provide comparably accurate predictions. BERTINI is generally closer to the experimental data for light targets, while INCL++ performs better on heavy targets, such as lead, which is most interesting for the present work and in general for spallation neutron sources.

3. Pions in the n_TOF spallation target

While thin-target cross sections can provide some indications on the ability of the models to correctly predict pion production, the structure of the hadronic showers that take place in the spallation target, and in particular the role played by secondary pions in the production of neutrons and photons, can only be studied by means of dedicated MC simulations of the spallation process and comparison with available experimental data. In this respect, we have chosen in this work to perform further simulations of the n_TOF spallation target with the Geant4 toolkit.

3.1. The Geant4 toolkit

Geant4 (GEometry ANd Transport) is a toolkit for the simulation of particle transport and detector response [5,6]. Physics models in Geant4 are organized and collected in "physics lists" (PL), which are specifications of the physical processes (and the associated models) that should be used in the simulation. The names of the available Geant4 PL are often obtained by concatenating the names of the models used in the hadronic sector, in decreasing order of incident energy. Thus, for instance, the FTFP_INCLXX_HP physics list, around which much of the present work revolves, relies on the Fritiof+pre-equilibrium model (FTFP) at high energy, the INCL++ model at intermediate energies, and the HP model at low energy. This work is based on Geant4 version 10.1; however, the INCL++ model within Geant4 was manually upgraded to version 5.2.9.4, which is the version that has been distributed with Geant4 version 10.2 (December 2015).

3.2. The n_TOF simulation

The n_TOF spallation target is a water-cooled lead cylinder surrounded by an aluminum container and by a neutron moderator. Its structure is described in detail in Refs. [2–4]. A 20-GeV/c proton beam impinges on the base of the lead cylinder at an angle of approximately 10°. The lead target cylinder can be considered as thick, in the sense that its size (radius 30 cm, length 40 cm) is large compared to the proton mean free path for inelastic collisions at the beam energy (∼ 15 cm).

In Ref. [3], Geant4 simulations of neutron production at the n_TOF spallation target, performed with several PL, were compared between each other and to the energy-differential neutron fluence measured at n_TOF in various experimental campaigns. It was shown that the lists based on the INCL++ model closely reproduce the energy dependence of the neutron spectrum and, within a 15–20% difference, the integrated yield. All other models are able to reproduce the shape, but overestimate the yield by a larger factor, of up to 70%.

Several tests were performed with Geant4 simulations in order to understand the origin of the differences among the available intra-nuclear cascade models for neutron and prompt-photon production. In order to shed some light on the mechanisms that leads to the production of photons, we have performed simulations by inhibiting

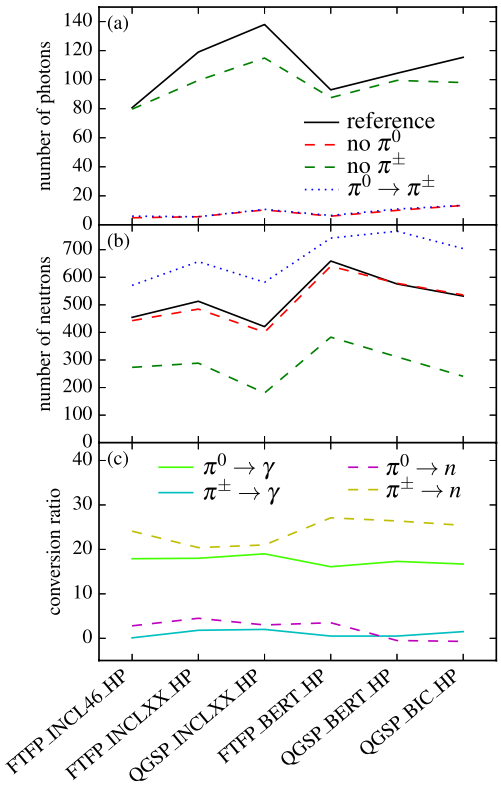

Figure 3. Number of photons (a) and neutrons (b) in the test calculations as a function of the physics list used. Panel (c) represents the pion-to-particle conversion ratios.

π^0 decay; this allows to establish how often prompt photons originate, either directly or through secondary electromagnetic cascade, from π^0 decay. A few low-statistics test runs were performed with different physics lists. The results of these simulations are shown in Fig. 3. All numbers are normalized to the number of incident protons. Several considerations can be made on the basis of the results in Fig. 3.

First, at least 90% of the prompt photons descend in some way from π^0 decay. This is clearly indicated by the effect of the suppression of π^0 decay in all the physics lists, but also by the observation that physics lists predicting large π^0 production rates typically also predict larger numbers of photons.

Second, the influence of π^0 decay on neutron production is sensibly smaller and of the order of a few percent only. This is easily understood because the coupling from photon transport to neutron transport is weaker; the $\gamma \to$ n photo-nuclear conversion is in general quite inefficient at producing neutrons, compared to pion-induced reactions. The results in Fig. 3 clearly hint to a fundamental role of pion production in general, and π^0 production in particular, in determining the final neutron and photon fluences in spallation neutron sources based on high-energy protons impinging on large spallation volumes.

In summary, it is quite clear that neutral pions dominate the production of prompt, high-energy photons. At the same time, the observed anti-correlation of neutron and prompt-photon yields can be explained considering that neutral pions essentially divert energy from the hadronic cascade towards the electromagnetic one.

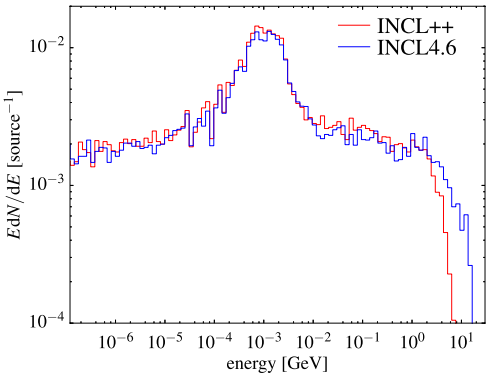

Figure 4. Neutron spectrum per unit lethargy emitted from the n_TOF spallation source in a 2° cone directed towards the first experimental area, as calculated by our Geant4 simulation. Results are shown for the INCL model with (INCL++) and without (ICL4.6) multipion extension.

3.3. Influence of pion multiplicity

It is also instructive to study the dependence of the calculation results on the mean pion multiplicity in individual nuclear reactions. By acting on some internal model parameter, one could modify the average pion multiplicity while keeping the overall coherence of the model. For this purpose, we shall discuss calculations performed with INCL++ with and without multipion extension. Figure 4 shows the calculated neutron fluence per unit lethargy and per incident proton emitted from the spallation source in the direction of the first experimental area. This spectrum is scored at the exit of our geometry and we only consider neutrons within a 2° cone around the direction towards EAR1. It is immediately obvious that the difference between the two models is small, so the global effect of the multipion extension on the neutron yield is of the order of a few percent. The neutron spectra are essentially identical in shape up to about ~ 1 GeV. Neutrons above 1 GeV are seen to be more abundantly produced by INCL4.6. This is coherent with the fact that higher pion multiplicities lead to more efficient dissipation of the projectile energy; clearly, it is easier to produce high-energy neutrons if less energy is channeled into pion production. Figure 5 compares the results of INCL4.6- and INCL++-based calculations on prompt-photon production. We apply the same 2° angular cut on the angle of the emitted photon; in addition, we only select photons that are emitted within 100 ns from the beam pulse. This roughly corresponds to the prompt photons that are detected before 1 μs at the EAR1 experimental area [3]. The difference between the calculations is much larger than for neutrons, especially for the production of high-energy photons. This is not surprising, given the crucial role that neutral pions are seen to play in the production of prompt high-energy photons. The results shown above indicate that the pion multiplicity in a single nucleon-nucleon or pion-nucleon collision does not play a crucial role in neutron and photon production in thick spallation targets. This property has already been observed at lower energies [17]; our work confirms that it still holds at n_TOF energies. Of course, the insensitivity of the outgoing energy to the details of the model is partly a trivial consequence of the fact that energy and momentum are conserved in both cases. On a geometric scale larger than the reaction mean free path, the

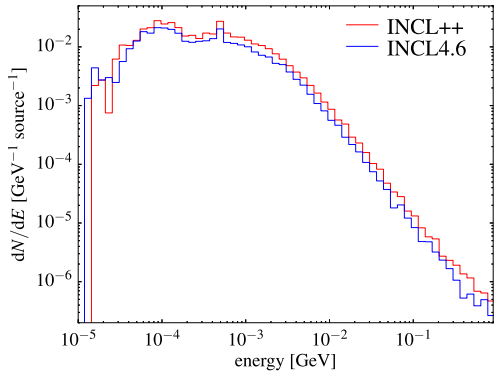

Figure 5. Photon spectrum emitted from the spallation source within 100 ns of the beam pulse, in a 2° cone directed towards the first experimental area, as calculated by our Geant4 simulation. Results are shown for the INCL model with (INCL++) and without (INCL4.6) multipion extension.

overall structure of the resulting hadronic cascade will be relatively independent of the details of the model. In other words, the number of neutrons and photons produced in the full hadronic cascade (and therefore the fluence of particles emerging from the spallation target) will mostly depend on the total number of pions (and other intermediate particles) produced in the cascade, rather than on their multiplicity in each reaction.

4. Conclusions

The role of pion production in spallation reactions has been further investigated by performing dedicated Geant4 simulations of the n_TOF spallation target. As suggested in Ref. [3], models producing overall more pions per incident proton also produce fewer neutrons, with a clear anti-correlation effect. On the contrary, prompt γ-rays, which are mostly produced by electromagnetic cascade following π^0 decay, correlate with the total number of pions in the hadronic cascade. This observation points out to a fundamental role of π^0 production in determining both the final neutron and γ-ray fluence produced by a spallation source based on high-energy protons on a heavy target.

It has been further observed that, contrary to the thin-target case, the previous INCL version leads to thick-target neutron and photon productions that are not sensibly different from the new version, except for very high-energy neutrons (above a few GeV). This finding has been related to the structure of the whole hadronic cascade that develops in a thick spallation target; the emitted particles are shown to be sensitive only to the total number of pions produced along the hadronic cascade, in particular neutral pions. The mitigated dependence of thick-target yields on the underlying elementary cross sections is a direct consequence of conservation laws, and applies only for dimensions of the spallation target sensibly larger than the mean free path of secondary particles, as in the case of the n_TOF target considered in this work.

References

[1] D. Filges, *Handbook of spallation research. Theory, experiments and applications* (Wiley- VCH, Berlin, 2009)
[2] C. Guerrero, et al., Eur. Phys. J. A **49**, 27 (2013)
[3] S. Lo Meo, et al., Eur. Phys. J. A **51**, 160 (2015)
[4] J. Lerendegui, et al., Eur. Phys. J. A **52**, 100 (2016)
[5] S. Agostinelli, et al., Nucl. Instrum. Meth. A **506**, 250 (2003)
[6] J. Allison, et al., IEEE T. Nucl. Sci. **53**, 270 (2006)
[7] A. Boudard, et al., Phys. Rev. C **66**, 044615 (2002)
[8] D. Mancusi, et al., Phys. Rev. C **90**, 054602 (2014)
[9] J. M. Quesada, et al., Prog. Nucl. Sci. Technol. **2**, 936 (2011)
[10] J.-J. Gaimard, et al., Nucl. Phys. A **531**, 709 (1991)
[11] A. Junghans, et al., Nucl. Phys. A **629**, 635 (1998)
[12] M.G. Catanesi, et al., HARP Collaboration), Phys. Rev. C **77**, 055207 (2008)
[13] M. Apollonio, et al., (HARP Collaboration), Phys. Rev. C **80**, 065207 (2009)
[14] D. Wright, et al., Nucl. Instrum. Meth. A **804**, 175 (2015)
[15] G. Folger, et al., Eur. Phys. J. A **21**, 407 (2004)
[16] A. Boudard, et al., Phys. Rev. C **87**, 014606 (2013)
[17] T. Aoust, et al., Phys. Rev. C **74**, 064607 (2006)